ANALYTICAL IDENTIFICATION OF BLADE-VORTEX INTERACTION NOISE CONTROLLER SUITED FOR MINIATURE TRAILING EDGE EFFECTORS

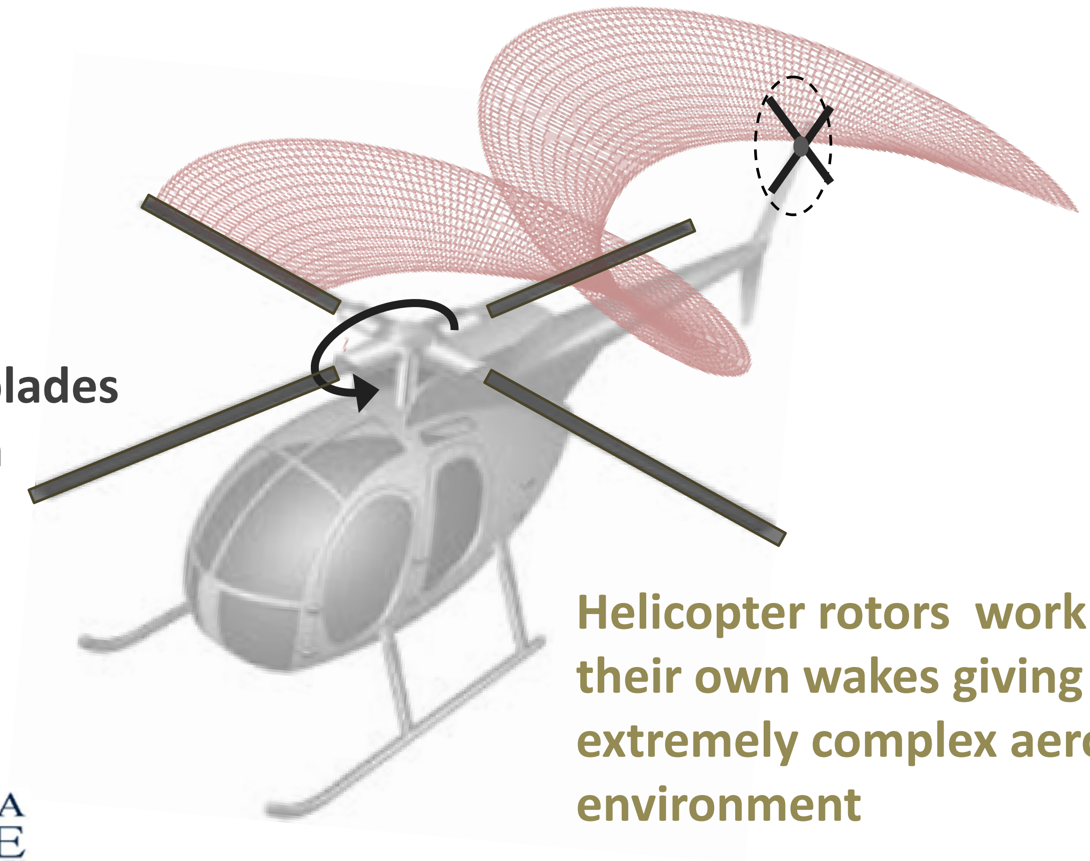

Slender elastic blades in rotary motion

Helicopter rotors work very close to their own wakes giving rise to an extremely complex aeromechanical environment

ENAC
ENTE NAZIONALE PER L'AVIAZIONE CIVILE
ITALIAN CIVIL AVIATION AUTHORITY
ROMA TRE
UNIVERSITÀ DEGLI STUDI

Fluid-structure interactions generate structural vibrations and noise pollution

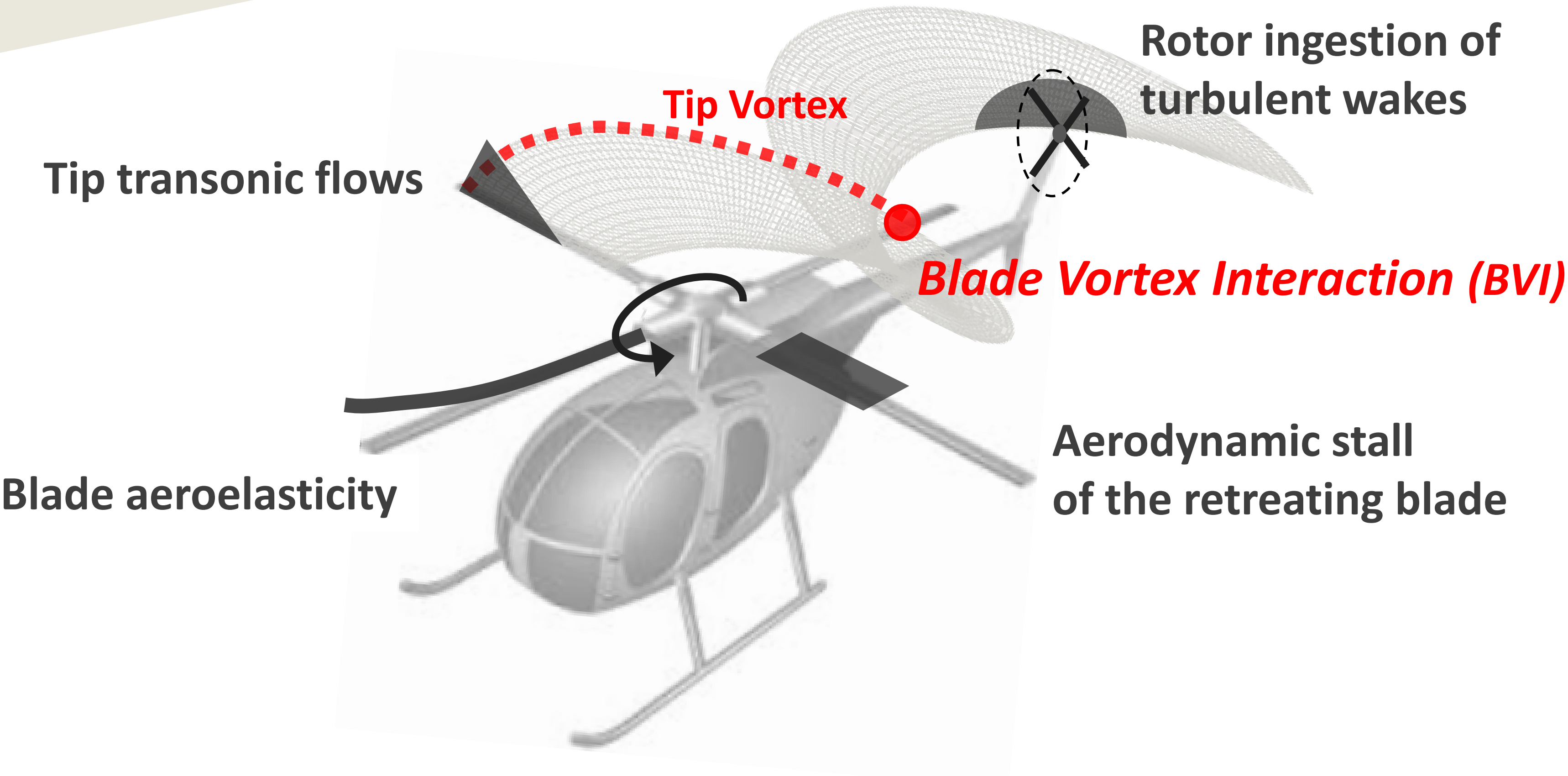

HELICOPTER NOISE CONTRIBUTIONS

Ingestion of Turbulent Wake
Broadband Noise

Tip Transonic Flows
High-speed Impulsive Noise

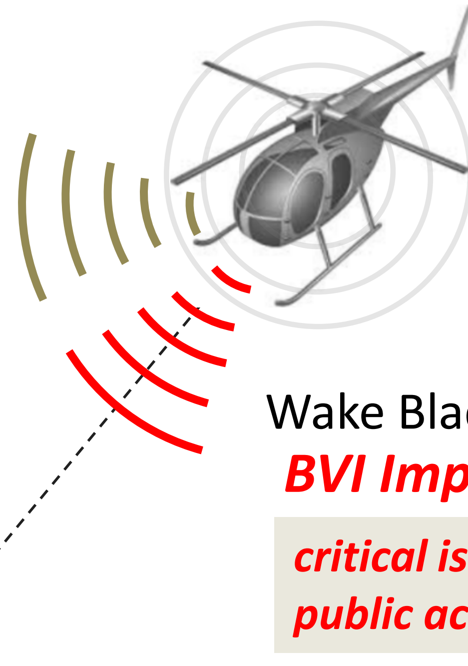

Occurring during landing operations in proximity of urban populated areas

Harmonic content on the human ear sensitivity range

Downward radiation pattern

Wake Blade Interactions
BVI Impulsive Noise

critical issue for helicopter public acceptance

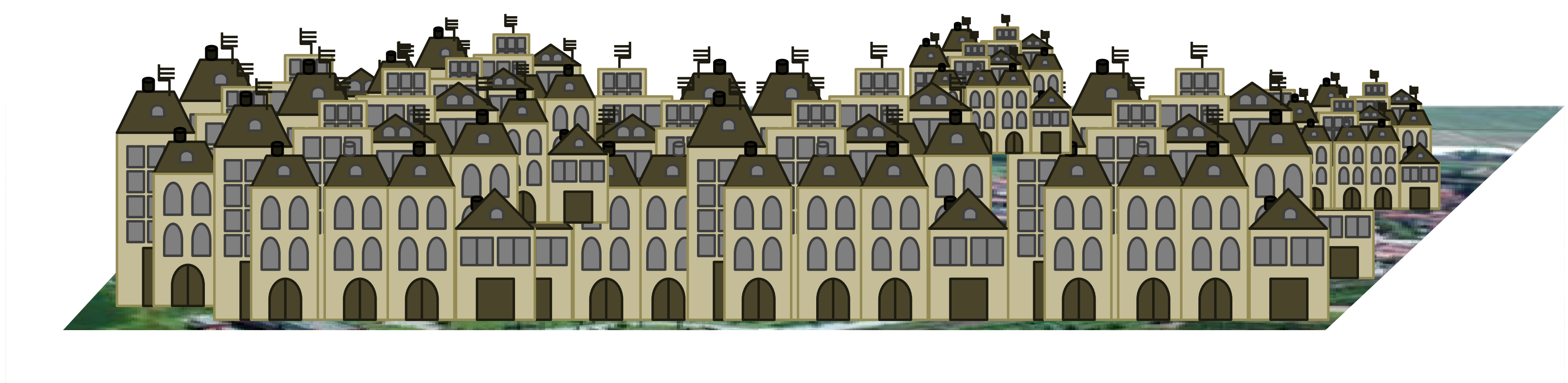

THE COMPUTATIONAL TOOLS

BVI SCENARIO CAPTURING

Potential rotor **BEM formulation**
suitable for BVI analysis

CONTROLLER SETTING

Analytical closed-loop control approach
based on **the Theodorsen theory**
suitable for **MITEs** actuation

BVI NOISE CONTROL

Farassat 1A formulation suitable for rotor
aeroacoustic analysis

BVI PHENOMENON INVESTIGATION

Main rotor aeromechanical environment allows for BVI events

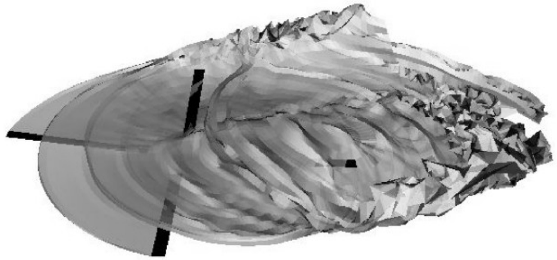

BVIs induce high frequency aerodynamic loads on main rotor blades

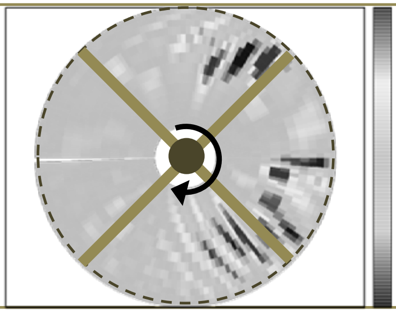

BVI loads act as acoustic sources of the emitted BVI impulsive noise

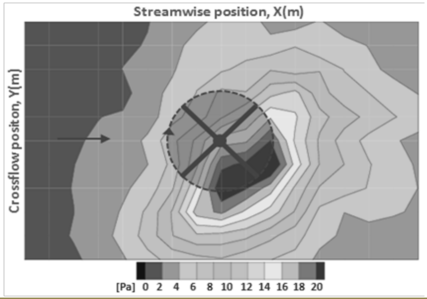

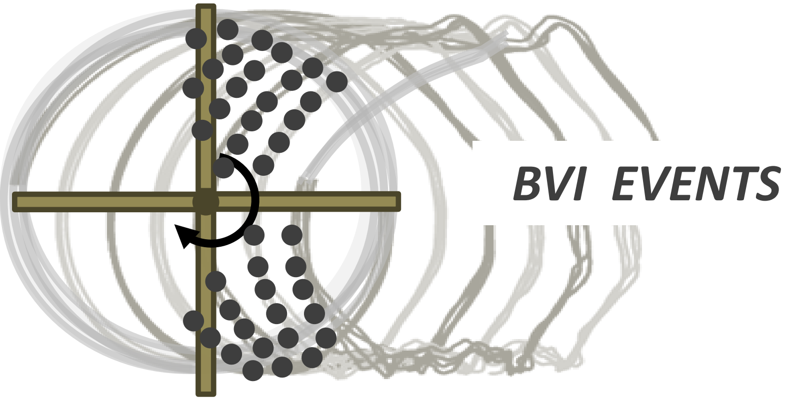

When tip vortices cross the rotor blades,
the velocity field induced on the surface is modified

BVI results into **impulsive aerodynamic loads** on the main rotor blades

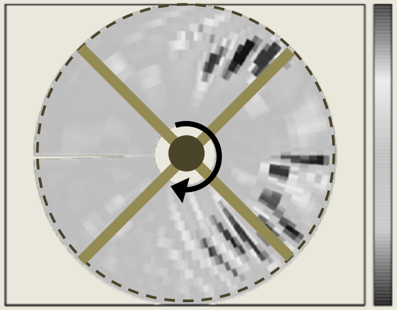

CONTROL DEVICE

HIGH HARMONIC
TIME-LOCALIZED CONTROL ACTION

TRAILING-EDGE FLAP

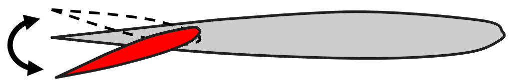

MICRO TRAILING EDGE EFFECTOR

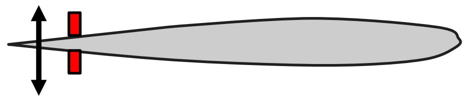

Low -Power Requirements and
Ease of Implementation

In the used potential-flow approach MITEs are replaced by suitable trailing-edge flaps providing equivalent aerodynamic responses

CONTROLLER AERODYNAMIC EFFECTS

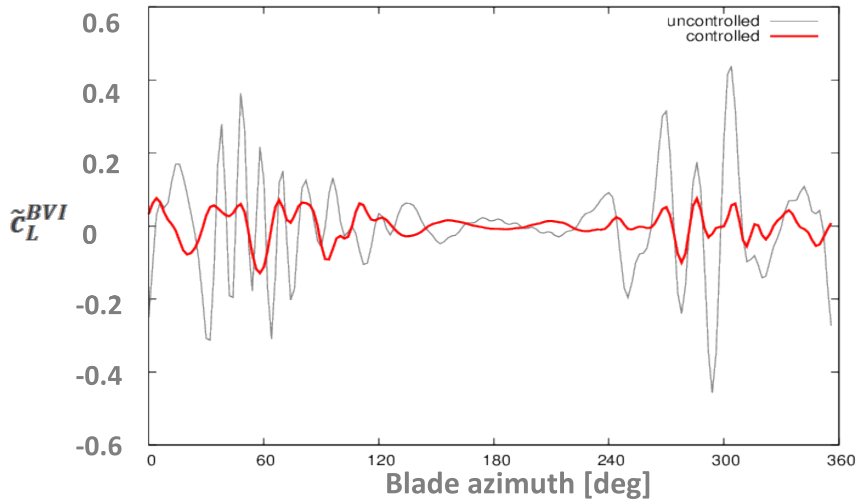

Control effectiveness to reduce rotor disk BVI loading

UNCONTROLLED

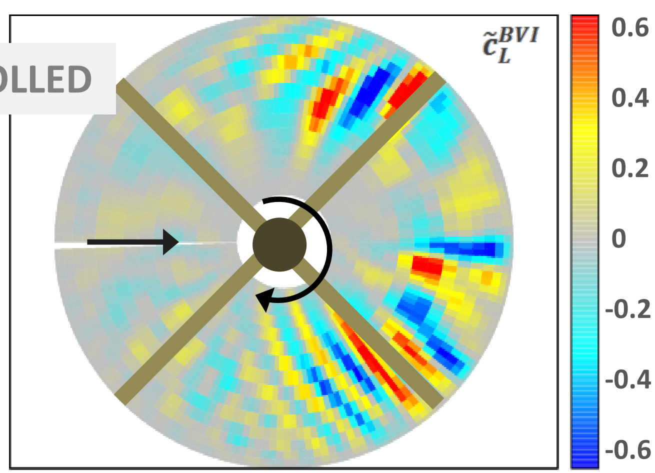

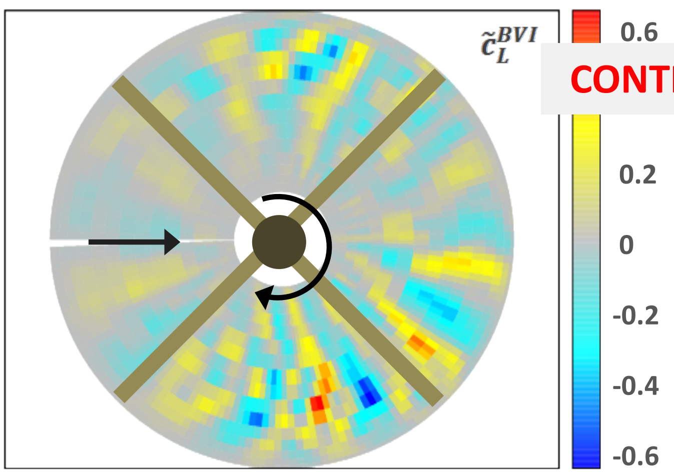

CONTROLLED

Control effectiveness to reduce BVI noise sound pressure levels (BVISPL)

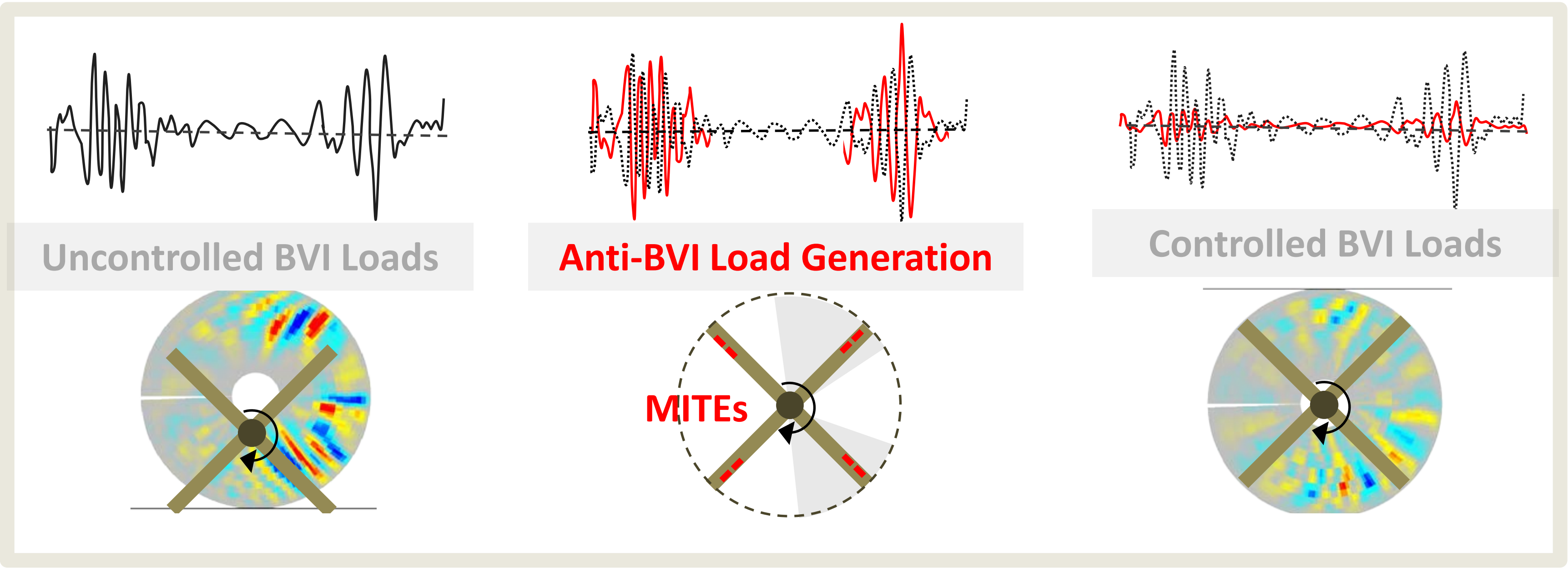

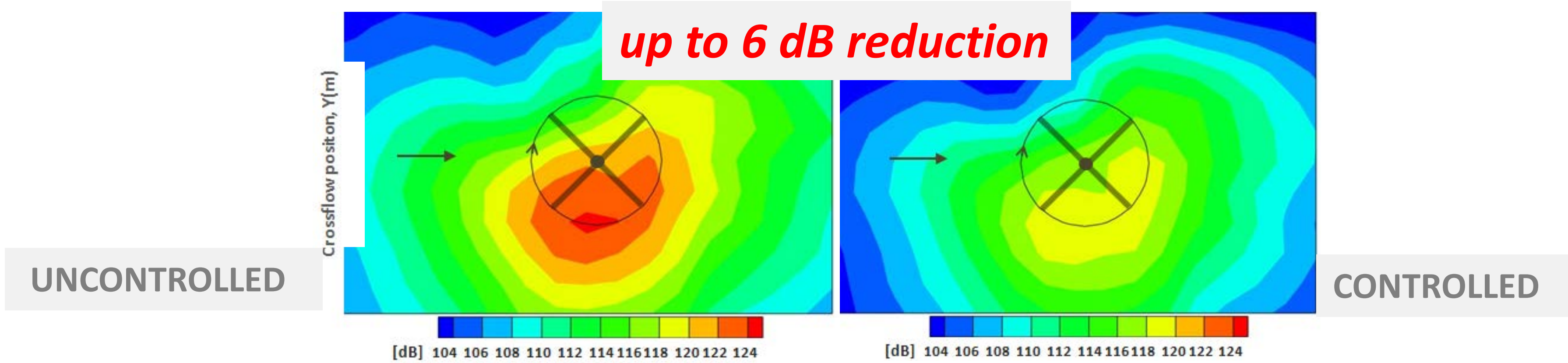

Hydroelasticity in sloshing tank and wave impact for shallow water condition: experimental and numerical study

Hydroelastic effects on elastic structure due to wave impact of sloshing flow in shallow water condition

- Topic related to LNG ship's tanks in low filling condition
- Pressure loads localized in space and characteristic time scales closed to the lowest natural period of the
- Ensure crew safety & avoid environmental disasters
- Description of the behavior of wave impact typologies, to understand the main features which can be relevant to trigger hydroelastic phenomena.

Marine Technology Research Institute
INSEAN

Effects of hydroelasticity, Euler and Cavitation numbers, differences between impact against rigid and elastic structure

Highlight the main physical aspects that play a significant role during the phenomenon evolution.

Build analitycal/numerical tools for an efficient and accurate description of the phenomenon

Two approaches to the problem:

Experimental test Numerical Simulation

Experimental activity:

- 2D tank excited by a sinusoidal sway motion

- 2 kinds of impact:
1. Flip-Through
2. Entrapment of a single air bubble

- Different ullage pressure for impact with air entrapment

- Deformable alluminium plate with strain gauges installed

- Rigid alluminium plate with pressure transducers installed

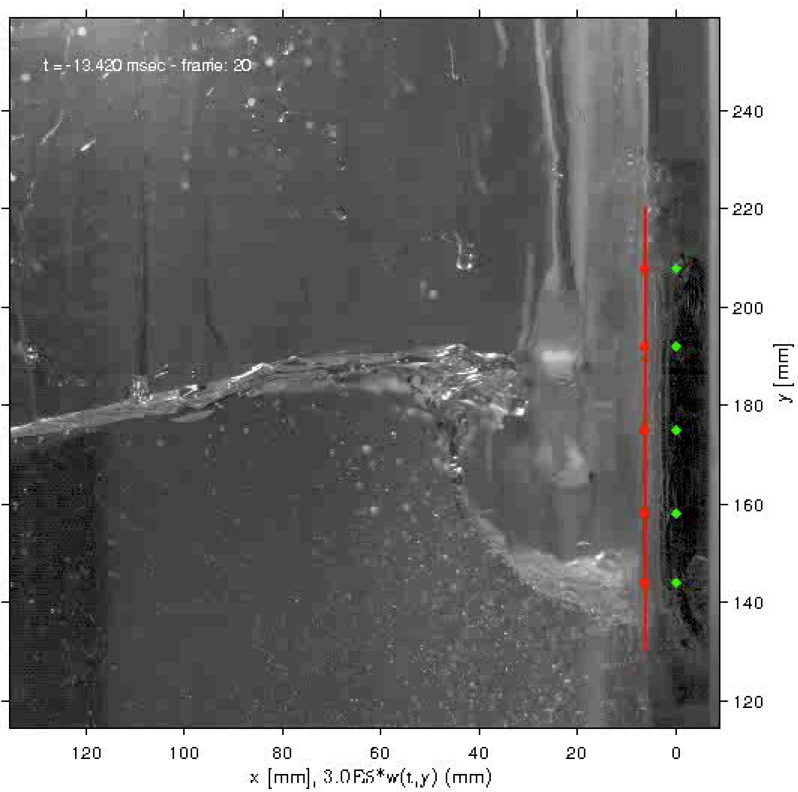
t = -13.420 msec - frame: 20
y [mm]
240
220
200
180
160
140
120
120
100
80
60
40
20
0
x [mm], 3.0E5*w(t,y) (mm)

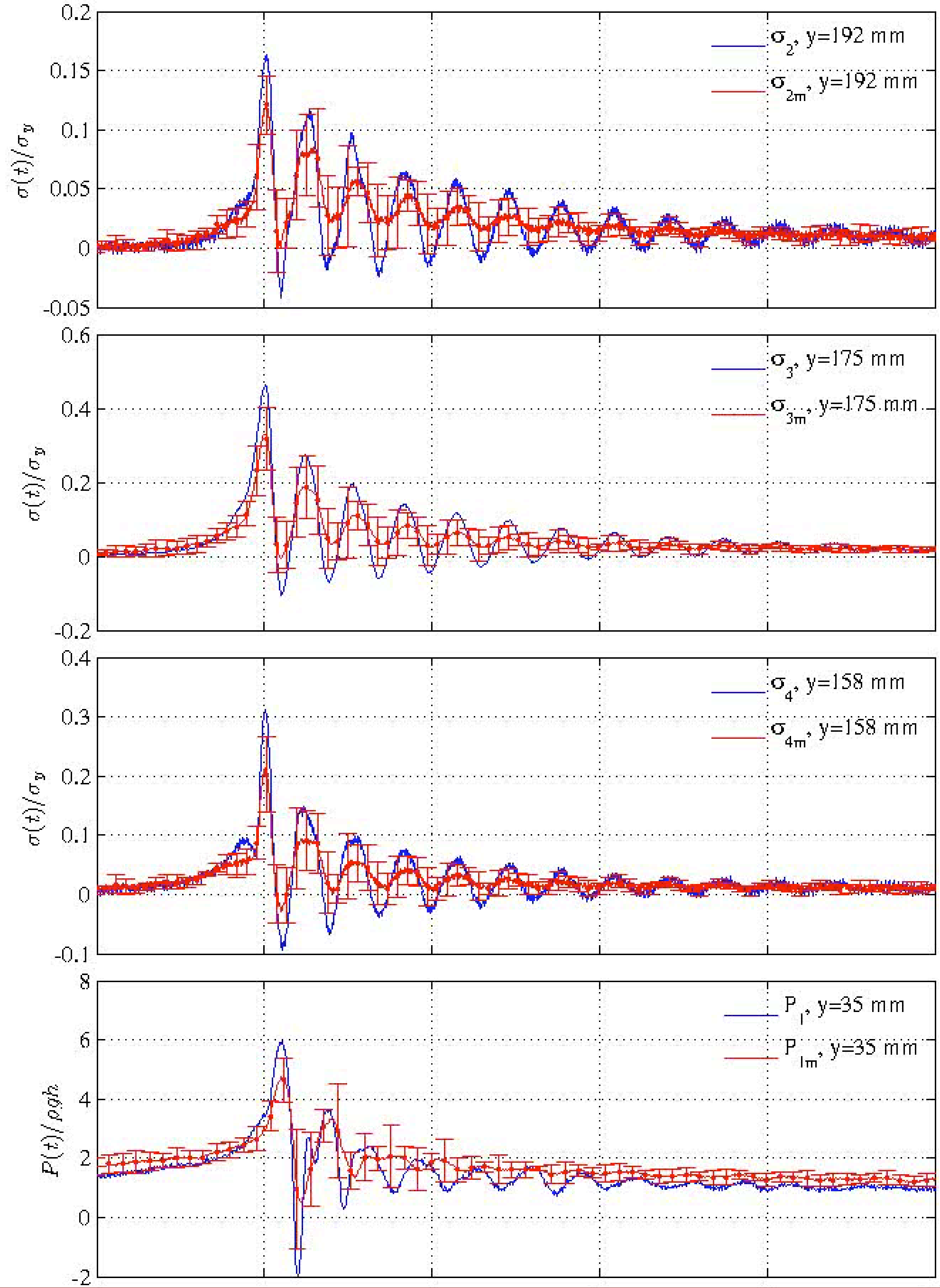
σ_2, y=192 mm
σ_{2m}, y=192 mm
$\sigma(t)/\sigma_y$
0.2
0.15
0.1
0.05
0
-0.05
σ_3, y=175 mm
σ_{3m}, y=175 mm
$\sigma(t)/\sigma_y$
0.6
0.4
0.2
0
-0.2
σ_4, y=158 mm
σ_{4m}, y=158 mm
$\sigma(t)/\sigma_y$
0.4
0.3
0.2
0.1
0
-0.1
P_1, y=35 mm
P_{1m}, y=35 mm
$P(t)/\rho gh$
8
6
4
2
0
-2

Harmonic Polynomial Cell (HPC) numerical scheme

- Incompressible, inviscid and irrotational flow for water
- Fully nonlinear boundary conditions for the free surface
- Potential flow theory & fully non-linear mixed Eulerian-Lagrangian formulation for the free surface boundary condition.

4^{th} order accurate, sparse matrix, easy parallelization $\longrightarrow$ Efficient algorithm (memory usage, cpu time)

Discretization of the doman with structured mesh (quadrilateral element): 2D and 3D

Harmonic Polynomial Cell (HPC) numerical scheme

The solution is approximated by a linear combination of harmonic functions

$$\Delta F(x,y) = Q(x,y) + B.C.$$

Solution defined as:

$F(x,y) = f_i(x,y)c_i + g_j(x,y)d_j$ $\quad i=1..8,\ j=1..9$ (Einstein notation for indices)

$\Delta f_i(x,y)c_i=0,$ $\quad f_i\,(x,y)$ harmonic functions

The domain is discretized in quadrilateral elements.

Each point associated to stencil formed by 4 quadrilateral neighboring elements and 8+1 grid points.

The approximate solution is evaluated on the boundary nodes (1-8) to express the unknown coefficients b_i

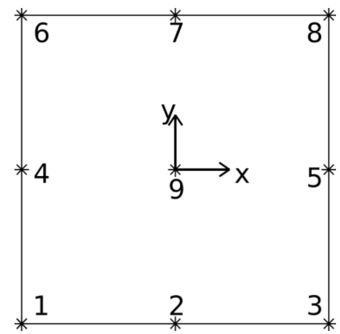

Stencil associated to a generic computational point

Laplace (I)

Potential Flow with
Nonlinear Free Surface:
Wavemaker Problem

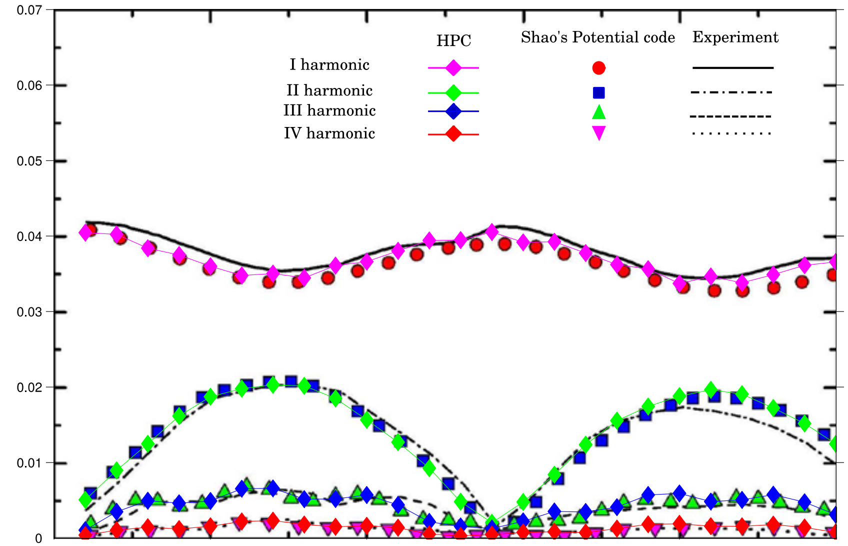

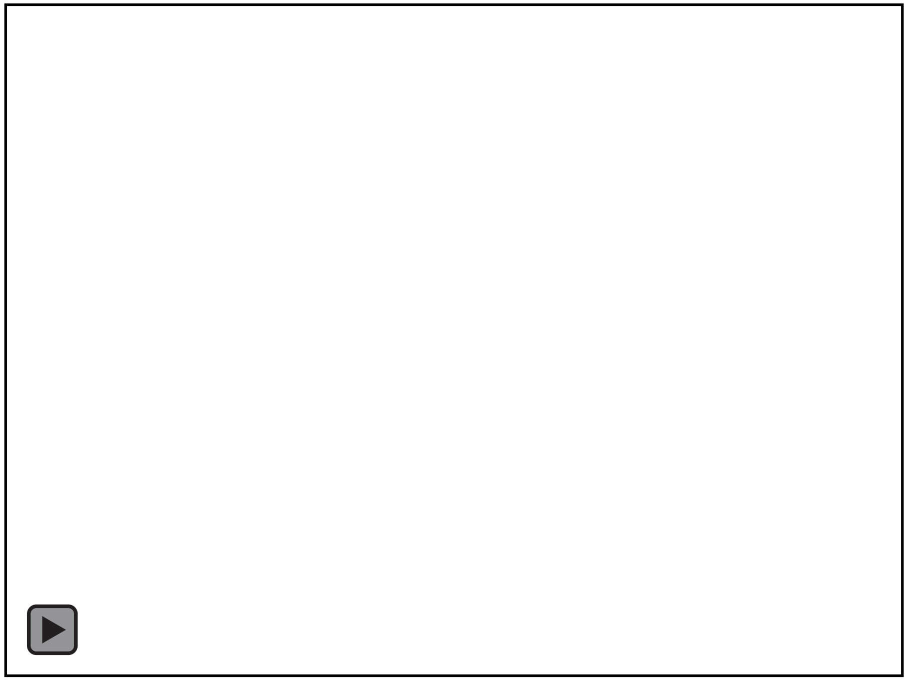

Laplace (II)

Potential Flow :
Impact problem in sloshing flow
Flip-through

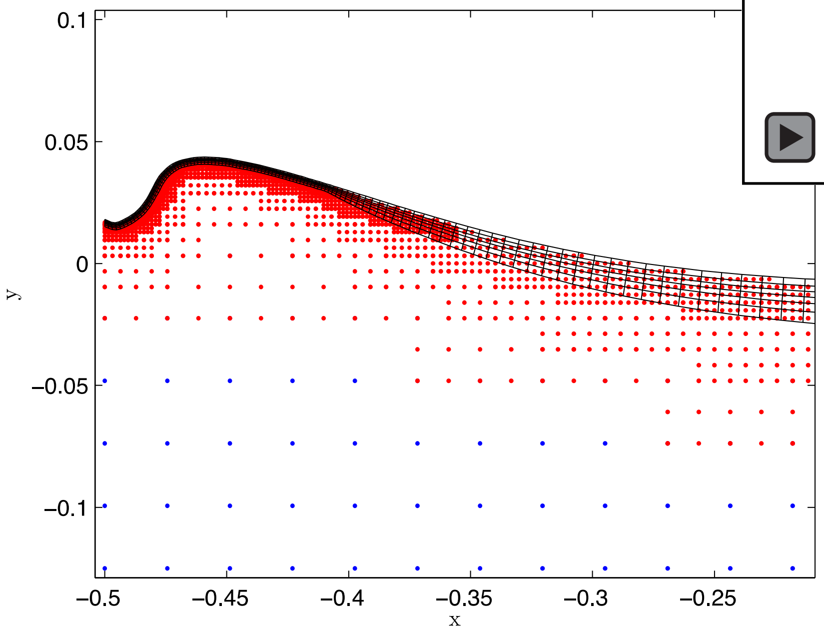

Implementation of
Adaptive Mesh Refinement:
background grid (blu dots),
mesh refinement(red dots),
free-surface fitted grid (black line)

Incompressible N-S solver

HPC coefficient matrices as set of discrete differential operators to solve generic differential problems: Navier-Stokes eq.

- e.g. Flow around cylinder, Re = 40

  Polar coordinates - $R_{dom}/D = 22$

  Euler scheme for time integration, C = .16

  Expected accuracy $O(\mathrm{d}x^4, \mathrm{d}t)$

Incompressible N-S solver

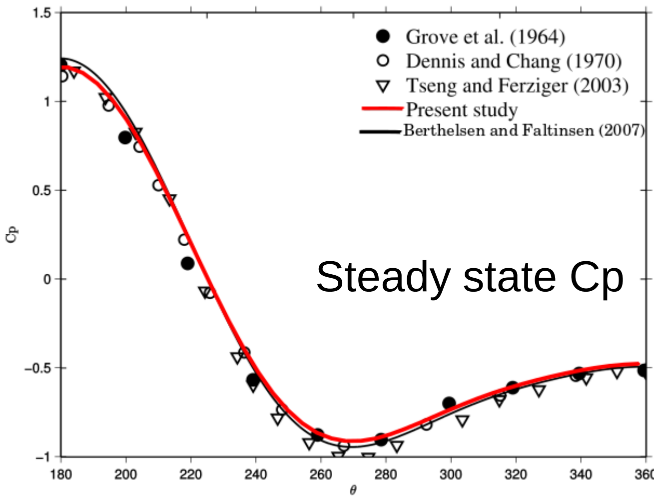

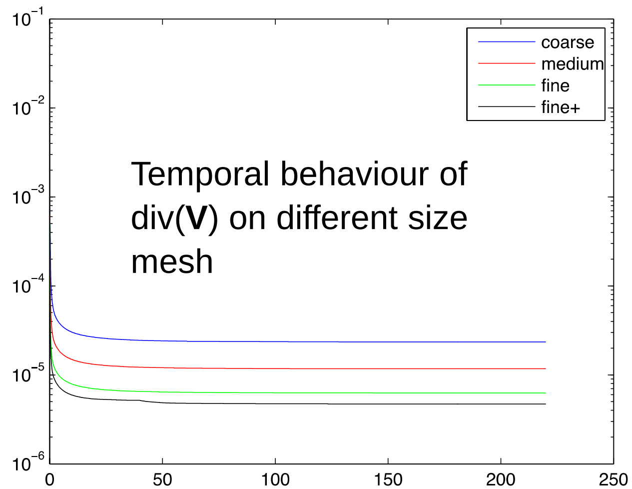

Convercenge of div(**V**) ($\Delta\text{e}^{3.3}$)

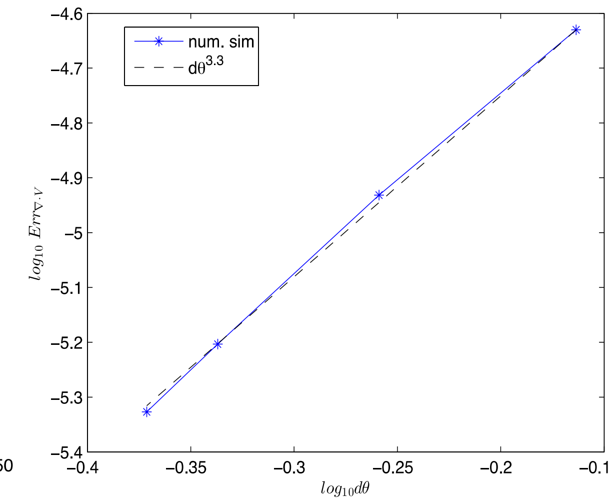

Velocity field at steady state (t = 220 sec):
Comparison of vortex center (green dot), length (purple dot) and separation point (red dot). Black line: Berthelsen and Faltinsen (2007)

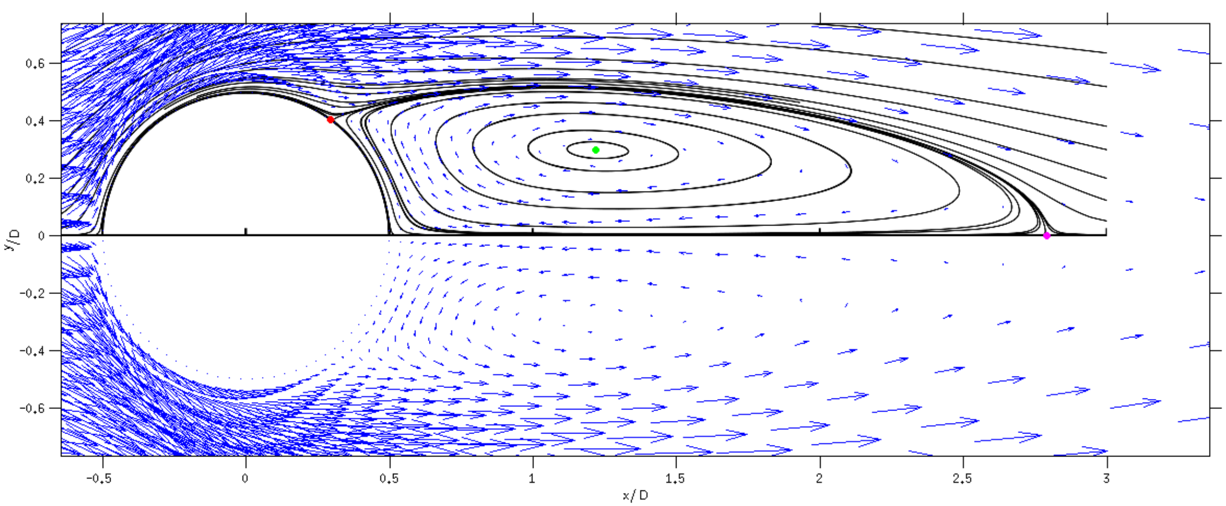

Convercenge of KE ($\Delta\text{e}^{2.45}$)